

# Dual-Band Unequal Wilkinson Power Divider with High Power-Dividing Ratio

Fang-Yu Lei, Yi-Hsin Pang, and Ming-Cheng Liang

Department of Electrical Engineering, National University of Kaohsiung, Kaohsiung 811, Taiwan

**Abstract** - This paper presents the design of a dual-band unequal power divider with high power-dividing ratio. No reactive lump components are required. Cost and loss could be consequently reduced. For verification, a 2.45/5.8-GHz prototype with 16:1 power-dividing ratio was fabricated and measured. Simulated and measured results are consistent with each other.

**Index Terms** — Dual band, high power-dividing ratio, microstrip, unequal power divider.

## 1. Introduction

Unequal Wilkinson power dividers are key components in microwave circuits, such as antenna feeding networks for pattern synthesis. A single-band 15:1 power divider has been presented [1]. Transmission lines of moderate impedances along with series inductors/shunt capacitors are used to replace the quarter-wavelength ( $\lambda/4$ ) transformers in a traditional Wilkinson power divider. A single-band unequal power divider without reactive components has been proposed [2]. The power-dividing ratio which is not related on impedance of transmission lines can be arbitrary theoretically. Dual-band unequal Wilkinson power dividers have also been reported [3], [4]. In [3], a pair of T-shaped lines and two-section impedance transformers are utilized for dual-band operation. Power-dividing ratio is still limited. By replacing the transmission lines in [2] with composite right/left-handed transmission lines, dual-band unequal in-phase/out-of-phase power divider was presented in [4]. Reactive lump components are required.

In this paper, a dual-band unequal Wilkinson power with high power-dividing ratio (16:1) is presented. This design is a modification of previous works [2,4]. The reactive lump components are no longer needed in this modified design. As a result, the loss and distortion due to the lump components can be eliminated.

## 2. Design and Analysis

Fig. 1 is the proposed dual-band unequal power divider. It consists four T-shaped lines and one resistor of resistance  $R$ . Two of the T-shaped lines are formed by a transmission line of characteristic impedance  $Z_1$ , the center of which is tapped with a shorted stub of line impedance  $Z_{1s}$ .  $2\theta_1$  and  $\theta_{1s}$  are the electrical lengths of the series transmission line and shunt stub, respectively. The other T-shaped lines are composed of a transmission line of line impedance  $Z_2$ , the center of which is tapped with an open stub of line impedance  $Z_{2s}$ .  $2\theta_2$  and  $\theta_{2s}$  are, respectively, the electrical lengths of the series transmission line and shunt stub. The

proposed dual-band power divider could be derived from its single-band counterpart in [2] by replacing each transmission line section with its equivalent T-shaped line or cascaded T-shaped lines.

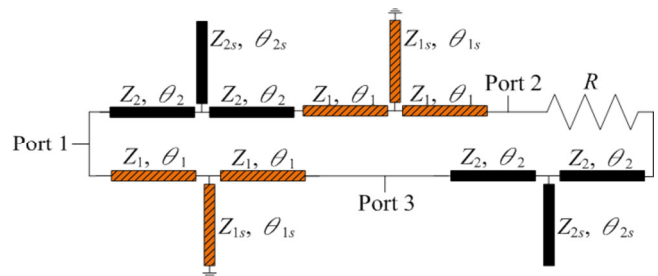


Fig. 1. Proposed dual-band unequal power divider.

### (1) Theory and Equations

Port impedance of  $Z_0 = 50 \Omega$  is assumed in this design. The T-shaped line is designed to be equivalent to a transmission line of impedance  $Z_c = \sqrt{2} Z_0$  and electrical length of  $+\phi - \phi$  at frequency  $f_1/f_2$ . For T-shaped lines with shorted and open stubs,  $\phi = 90^\circ$  and  $\cos^{-1}(1/k)$  are required, respectively, where  $k = |S_{21}/S_{31}| \geq 1$  is the square root of power-dividing ratio [2]. Comparing ABCD matrices of the T-shaped line and its equivalent transmission line, design equations of  $Z_1$ ,  $Z_2$ ,  $Z_{1s}$ , and  $Z_{2s}$  could be derived as:

$$Z_1 = \frac{\pm Z_c}{\tan \theta_1} \quad (1)$$

$$Z_{1s} = \frac{Z_1 \cdot \sin(2\theta_1)}{2 \cdot (2\sin^2 \theta_1 - 1) \cdot \tan \theta_{1s}} \quad (2)$$

$$Z_2 = Z_c \frac{\pm \tan(\phi/2)}{\tan \theta_2} \quad (3)$$

$$Z_{2s} = \frac{Z_2 \sin(2\theta_2) \cdot \tan \theta_{2s}}{2 \cos(2\theta_2) - \cos \phi} \quad (4)$$

The upper and lower signs in (1) and (3) are for frequencies  $f_1$  and  $f_2$ , respectively. For dual-band operation at  $f_1$  and  $f_2$ ,  $\theta_1, \theta_{1s}, \theta_2$  and  $\theta_{2s}$ , at the frequency of  $f_0 = (f_1 + f_2)/2$  should be selected as multiples of  $90^\circ$ . These angles should be as small as possible and carefully selected so that  $Z_1, Z_2, Z_{1s}$ , and  $Z_{2s} > 0$  are guaranteed. The cascaded T-shaped lines are then equivalent to a transmission line with impedance of  $\sqrt{2} Z_0$  and electrical length of  $90^\circ + \phi$  and  $-90^\circ - \phi$  at  $f_1$  and  $f_2$ , respectively. According to the analysis in [4], the proposed circuit is a dual-band power divider with power-dividing ratio of  $k^2$ . For good isolation,  $R = 2Z_0$  is chosen [4].

### (2) Discussion on achievable power-dividing ratio

It is noticed that the values of  $Z_2$  and  $Z_{2s}$  depends on  $k$ . In general, the realizable characteristic impedance of a

microstrip line lies in the range from  $20 \Omega$  to  $120 \Omega$ . If  $\theta_2 = 90^\circ$  and  $\theta_{2s} = 180^\circ$  at  $f_0$  are selected,  $k^2$  could be in the range from 2 to 20. High power-dividing ratio is sustained.

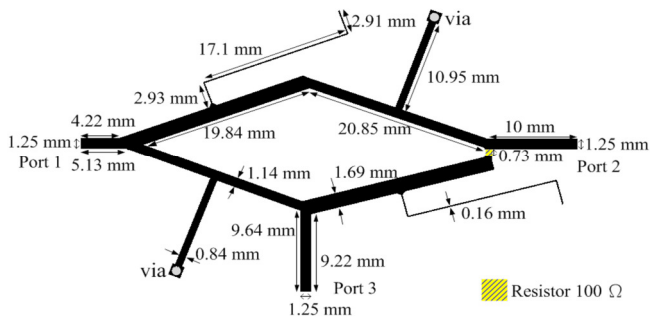


Fig. 2. Layout of the fabricated 16:1 power divider.

### 3. Experimental Results

A dual-band 16:1 ( $k = 4$ ) power divider is designed to operate at  $f_1/f_2 = 2.45/5.8$  GHz. It was implemented on a RO4003C substrate with a dielectric constant of 3.55 and thickness of 20 mils.  $\theta_1 = \theta_{1s} = \theta_2 = 90^\circ$  and  $\theta_{2s} = 180^\circ$  at 4.125 GHz are selected.  $Z_1 = 52.4 \Omega$ ,  $Z_{1s} = 63.85 \Omega$ ,  $Z_2 = 40.6 \Omega$ , and  $Z_{2s} = 118.12 \Omega$  are calculated from (1) – (4). Fig. 2 shows the layout of the power divider. Full-wave simulation was also performed with Keysight Momentum. Fig. 3 – 5 are return loss, port isolation, and power division ratio of the designed circuit. The measured return loss of Ports 1, 2, and 3 at  $f_1/f_2$  are 29.0/14.8 dB, 22.0/21.3 dB, and 31.3/8.2 dB, respectively. The 13-dB bandwidth of  $S_{11}$  is 34.6% and 7.5% at the first and second frequency bands, respectively. The measured isolation ( $1/|S_{32}|$ ) at  $f_1/f_2$  are 24.6/18.3 dB. The simulated power dividing ratio at  $f_1/f_2$  is  $|S_{21}/S_{31}| = 12.3/17$  dB, while the measured data is 15.3/10.1 dB. The discrepancy is caused by frequency shift, and is enlarged due to the poor flatness of power-dividing ratio. Fig. 6 shows the phase difference. The simulated phase imbalance at  $f_1/f_2$  is  $-0.17^\circ/0.57^\circ$ , while the measured imbalance is  $6^\circ/-5.77^\circ$ .

### 4. Conclusion

A dual-band unequal Wilkinson power divider with high power-dividing ratio has been presented and validated by measurement. No reactive lump elements are required. Agreement between the simulated and measured results was observed.

### Acknowledgment

This work was supported in part by Ministry of Science and Technology, Taiwan, R.O.C., under Grant MOST 104-2221-E-390-008-. The authors thank National Chip Implementation Center (CIC), National Applied Research Laboratories, Taiwan, R.O.C. for their support in simulation software.

### References

- [1] T. Zhang, W. Che, and Y.-C. Chiang, "A compact 15:1 unequal power divider using composite transmission lines," in *Proc. Asia Pacific Micro. Conf.*, vol. 1, Dec. 2015, pp. 1 – 3.
- [2] K.-K. M. Cheng and P.-W. Li, "A novel power-divider design with unequal power-dividing ratio and simple layout," *IEEE Trans. Microw. Theory Techn.*, vol. 57, no. 6, pp. 1589–1594, June 2009.
- [3] Y. Wu, Y. Liu, X. Zhang, J. Gao, and H. Zhou, "A dual band unequal Wilkinson power divider without reactive components," *IEEE Trans. Microw. Theory Techn.*, vol. 57, no. 1, pp. 216–222, Jan. 2009.
- [4] P.-L. Chi, T.-C. Hsu, and Y.-T. Yan, "Single-layer dual-band arbitrary power-dividing and in-phase/out-of-phase power divider," in *Proc. Asia Pacific Micro. Conf.*, vol. 1, Dec. 2015, pp. 1 – 3.

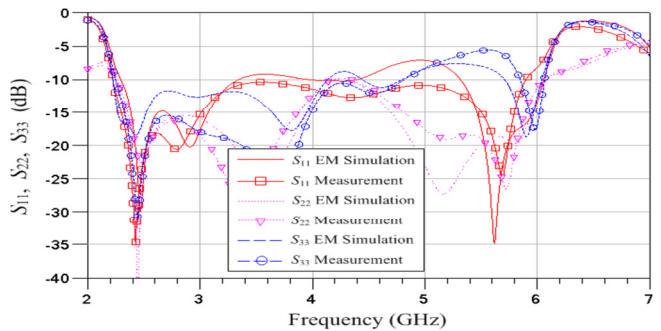


Fig. 3. Simulated and measured return loss.

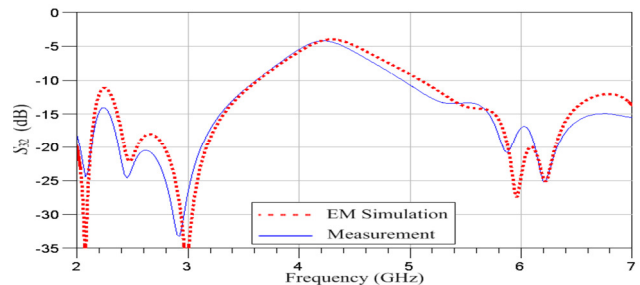


Fig. 4. Simulated and measured port isolation.

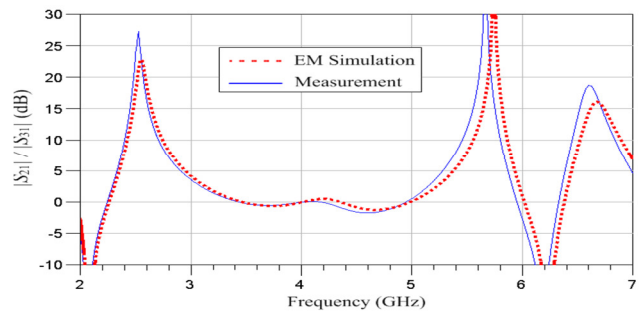


Fig. 5. Simulated and measured power-dividing ratio.

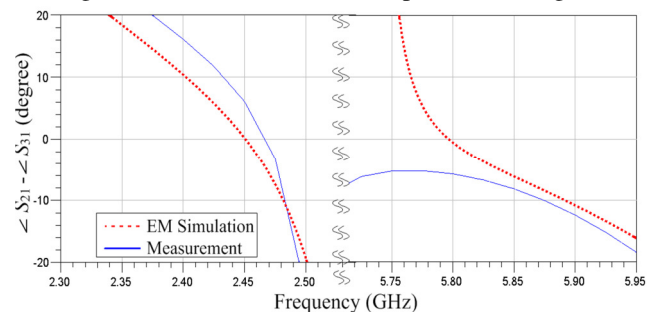


Fig. 6. Simulated and measured phase imbalance.